Vol 18 No 1, January 2009
1674-1056/2009/18(01)/0009-07

Chinese Physics B

© 2009 Chin. Phys. Soc.
and IOP Publishing Ltd

Approximate calculation of electronic energy levels of axially symmetric quantum dot and quantum ring by using energy dependent effective mass*

Liu Yu-Min(刘玉敏)†, Yu Zhong-Yuan(俞重远), and Ren Xiao-Min(任晓敏)

Institute of Optical Communication and Optoelectronics, Beijing University of Posts and Telecommunications, Beijing 100876, *China*
Key Laboratory of Optical Communication and Lightwave Technologies, Ministry of Education (Beijing University of Posts and Telecommunications), Beijing 100876, *China*

(Received 10 December 2007; revised manuscript received 25 August 2008)

Calculations of electronic structures about the semiconductor quantum dot and the semiconductor quantum ring are presented in this paper. To reduce the calculation costs, for the quantum dot and the quantum ring, their simplified axially symmetric shapes are utilized in our analysis. The energy dependent effective mass is taken into account in solving the Schrödinger equations in the single band effective mass approximation. The calculated results show that the energy dependent effective mass should be considered only for relatively small volume quantum dots or small quantum rings. For large size quantum materials, both the energy dependent effective mass and the parabolic effective mass can give the same results. The energy states and the effective masses of the quantum dot and the quantum ring as a function of geometric parameters are also discussed in detail.

Keywords: quantum dot, strain, quantum ring and electronic structure
PACC: 0365, 2110, 4620

1. Introduction

In recent years, much effort has been made to fabricate semiconductor quantum well, wire, and dot materials because of their great potential applications in semiconductor devices. The semiconductor quantum dots (QDs) are very attractive in optoelectronics applications such as QD laser, QD based photodetector and QD based semiconductor optical amplifier.[1−3] The semiconductor quantum rings (QRs) have become a central field due to their potential applications in quantum information processing.[4,5] The most popular methods to fabricate such quantum materials are based on the self-organized process by using the molecular beam epitaxy (MBE). It has been shown that various shapes of QDs and QRs can be fabricated in various experimental growth environments.[6] The shapes and the size distributions of QDs and QRs have been investigated intensively because of their importance in both the growth experiments and theoretical calculations of electronic structure.[7,8] The electronic structure calculations of the quantum materials have been conducted by using different methods based on the different schemes, such as effective mass approximation,[9] tight binding approximation[10] and pseudo-potential methods.[11] In the effective mass approximations, both the parabolic potential model and the parabolic effective mass model are often adopted. However, in such simplified models, the energy dependent effective mass is often ignored, for the problem can be solved in a simplified linear form.

In this paper, we investigate the electronic states of the axially symmetric cylinder shaped QDs. For the QRs, we consider their cross sections with rectangle, square, and elliptic shapes separately. In our simulations, the energy dependent effective mass approximation is adopted.

2. Physical model

We have studied the influence of strain and wetting layer on the energy states in the previous studies.[12−15] So in this study, we mainly investigate the dependences of energy states on the geometric shape, geometric size, and energy dependent effective

*Project supported by the National Basic Research Program of China (Grant No 2003CB314901), the National Natural Science Foundation of China (Grant No 60644004), and the High School Innovation and Introducing Talent Project of China (B07005).
†Corresponding author. E-mail: liuyumintech@hotmail.com

mass numerically. Both the strain effect and wetting layer are excluded from consideration in our simulation.

For the three-dimensional (3D) semiconductor heterostructure, the single-band envelope function in the effective mass approximation can be expressed as

$$\left[-\frac{\hbar}{2}\nabla\cdot\left(\frac{1}{m\left(E,\boldsymbol{r}\right)}\nabla\right)+V(\boldsymbol{r})\right]\psi\left(\boldsymbol{r}\right)=E\psi\left(\boldsymbol{r}\right), \quad (1)$$

where $\hbar$, $m\left(E,r\right)$, $V\left(r\right)$, E and $\psi\left(r\right)$ are Planck's constant divided by 2π, the position and the energy dependent electronic effective mass, the position dependent band-edge induced confinement potential energy, the electronic energy level and wavefunction, respectively. Since the quantum material model is rotationally symmetric, the wavefunction can be written as $\psi\left(r,z,\theta\right)=\varphi\left(r,z\right)\phi\left(\theta\right)$ by separating variables. V and m in Eq.(1) are azimuthal angle independent and can be expressed as $V=V\left(r,z\right)$ and $m=m\left(E,r,z\right)$). Equation (1) can be re-expressed as

$$\left[-\frac{\hbar^2}{2}\frac{\partial}{\partial z}\left(\frac{\partial\varphi\left(r,z\right)}{m\left(E,r,z\right)\partial z}\right)-\frac{\hbar^2}{2}\frac{1}{r}\frac{\partial}{\partial r}\left(\frac{r\partial\varphi\left(r,z\right)}{m\partial r}\right)\right]\phi\left(\theta\right),$$
$$\left[-\frac{\hbar^2\varphi\left(r,z\right)}{2mr^2}\frac{\partial^2}{\partial^2\theta}+V\left(r,z\right)\varphi\left(r,z\right)\right]\phi\left(\theta\right)=E\varphi\left(z,r\right)\phi\left(\theta\right). \quad (2)$$

Multiplying Eq.(2) with $\dfrac{mr^2}{\varphi\phi}$ leads to

$$\frac{mr^2}{\varphi}\left\{-\frac{\hbar^2}{2}\frac{\partial}{\partial z}\left(\frac{\partial\varphi\left(r,z\right)}{m\partial z}\right)-\frac{\hbar^2}{2r}\frac{\partial}{\partial r}\left(\frac{r\partial\varphi\left(r,z\right)}{m\partial r}\right)\right\}$$
$$+mr^2\left(V-E\right)=\frac{\hbar^2}{2}\frac{1}{\phi}\frac{\partial^2\phi}{\partial^2\theta}. \quad (3)$$

If we assume Eq.(3) to equal $-\dfrac{\hbar^2}{2}n^2$, the ϕ in Eq.(3) can be solved immediately as

$$\phi=\exp\left(\mathrm{i}n\theta\right), \quad (4)$$

where $n=0,\ \pm1,\ \pm2,\ \ldots$, are the electron orbital quantum numbers. Then the remaining parts of the Schrödinger equation turn into the following form:

$$-\frac{\hbar^2\partial}{2\partial z}\left(\frac{\partial\varphi\left(r,z\right)}{m\partial z}\right)-\frac{\hbar^2}{2}\frac{1}{r}\frac{\partial}{\partial r}\left(\frac{r}{m}\frac{\partial\varphi\left(r,z\right)}{\partial r}\right)$$
$$+\frac{n^2\hbar^2}{2mr^2}\varphi\left(r,z\right)+V\left(r,z\right)\varphi\left(r,z\right)=E\varphi\left(r,z\right). \quad (5)$$

The boundary conditions are as follows. For the up and down boundaries, the Dirichlet boundary conditions are used to ensure the wavefunction convergence. On the axis, $r=0$, and a special treatment should be noted: when $n=0$, or $\dfrac{\partial\varphi}{\partial r}=0$ due to the continuity, the Neumann boundary conditions are used; when $n\geq1$, however, to stop the item $\dfrac{n^2\hbar^2}{2mr^2}\varphi\left(r,z\right)$ approaching infinity (∞) at $r=0$, the Dirichlet boundary conditions should be used. From the mathematical point of view, model (5) combined with the boundary conditions turns into a partial differential equation (PDE) eigenvalue problem. The proposed model can greatly reduce the calculation cost by converting the 3D Schrödinger equation into a 2D problem. The equation can be solved by using the finite element numerical technique. Compared with the orthogonal periodic function expansion or Fourier expansion method, the finite element method has the advantage that it is independent of the geometry to be analysed. However, for the expansion method, one generally has to select the proper expansion functions to confirm the efficient convergent performance.

The energy and position dependent effective $m\left(E,r\right)$ is given by

$$\frac{1}{m\left(E,r\right)}=\frac{P^2}{\hbar^2}\left[\frac{2}{E+E_{\mathrm{g}}-V\left(r\right)}+\frac{1}{E+E_{\mathrm{g}}-V\left(r\right)+\Delta\left(r\right)}\right], \quad (6)$$

where P, E_{g} and $\Delta\left(r\right)$ represent the momentum matrix element, band gap and position dependent spin–orbit splitting in valence bands. The confinement potential $V\left(r\right)$ induced by the discontinuity of the conduction band edge at material interface between the QDs (or QRs) and the matrix barrier can be expressed as

$$V\left(r\right)=\begin{cases}0, & r\in\text{well materials},\\ V_0, & r\in\text{barrier materials}.\end{cases} \quad (7)$$

The Ben Daniel–Duke boundary conditions should be applied to the wavefunction at interface between well and barrier materials and can be expressed

as

$$\psi_{\text{well}}(r_{\text{s}}) = \psi_{\text{barrier}}(r_{\text{s}}) \frac{\hbar^2}{2m(E, r_{\text{s}})} \nabla_n \psi_{\text{well}}(r_{\text{s}}) = \frac{\hbar^2}{2m(E, r_{\text{s}})} \nabla_n \psi_{\text{barrier}}(r_{\text{s}}), \quad (8)$$

where r_{s} denotes the position on the interface and n refers to the normal direction of the interface. It can be seen that all these boundary conditions are dependent on the electron energy stats and material parameters.

From Eq.(5) it follows that the equation is a nonlinear equation, for the effective mass parameter m is dependent on the energy eigenvalue to be solved. In order to obtain the final convergent solution of Eq.(5), the nonlinear iteration scheme will be necessary for numerical calculations. First, we set an initial guess of energy as E_0, and then the effective mass $m(E, r)$ can be calculated based on Eq.(6). Second, the energy eigenvalue is obtained by solving Eq.(5). Third, the effective mass $m(E, r)$ is repressed by using the calculated E, and then the program goes back to the second step to form a complete loop. When the calculated energy eigenvalue converges to a stable value, the iteration is terminated. In solving Eq.(5), a finite element method is used to find the energy eigenvalues.

3. Results and discussion

For the InAs/GaAs materials, we use the following band structure parameters: the band gap of InAs ($E_{\text{g,InAs}}$) is 0.42 eV, i.e. $E_{\text{g,InAs}} = 0.42$ eV; the spin–orbit splitting energy of InAs for the valence band (Δ_{InAs}) is 0.48 eV, i.e. $\Delta_{\text{InAs}} = 0.48$ eV; the momentum matrix element of InAs is related to the expression $3m_0 P^2_{\text{InAs}}/\hbar^2 = 22.2$ eV, where m_0 is the free electron mass. The corresponding parameters of GaAs are $E_{\text{g,GaAs}} = 1.52$ eV, $\Delta_{\text{GaAs}} = 0.34$ eV and $3m_0 P^2_{\text{GaAs}}/\hbar^2 = 24.2$ eV. The conduction band offset (V_0) is taken as 0.77 eV, i.e. $V_0 = 0.77$ eV. Figure 1 shows the geometric shapes of the cylindrical quantum dot and elliptical quantum ring. Because of the axial symmetry, we show only half of the cross section. The quantum dot growth direction is along the z-axis. For quantum ring, r represents the inner radius, while R denotes the radius of the quantum ring cross-section and h is the height.

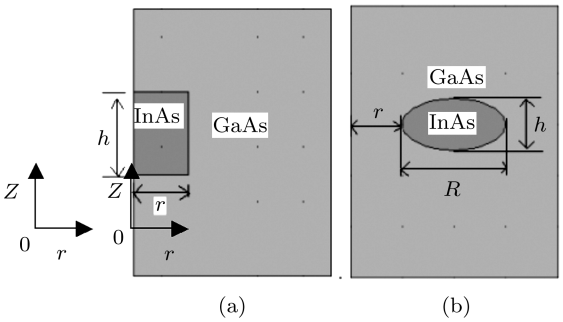


Fig.1. Schematic diagrams for axially symmetric cylinder shaped quantum dot (a) and elliptical quantum ring (b).

First of all, we show the efficient of the iteration numerical algorithm in solving the nonlinear problem. Figure 2 shows the typical convergent characteristics in the iteration calculations. As can be seen, the energy eigenvalue will be convergent to a relatively stable value after 6 iterations.

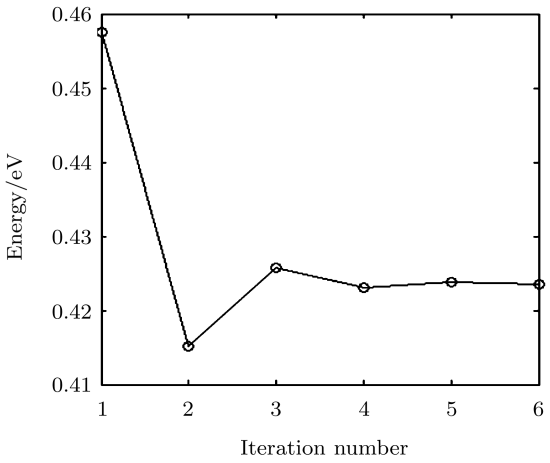


Fig.2. The typical convergent characteristics of the ground state energy level versus number of iterations.

Figure 3 (a) shows the ground state energy levels of the cylindrical quantum dots when the heights are 5 and 2.5 nm respectively. Both the non-parabolic mass approximation and the parabolic effective mass approximation are considered. For the parabolic effective approximation, we use the bulk effective mass $m(0)$ to replace the energy dependent effective mass $m(E)$. The bulk effective masses of the InAs and GaAs are 0.023 and $0.067m_0$ respectively. As demonstrated in Fig.3(a), the ground state energy level is very sensitive to the size of quantum dots. Compared with the energy dependent effective mass model, the ground state energy levels are overestimated by using the simplified parabolic effective mass model, especially when the radius of the quantum dot is less than 10 nm. For example, when the radius is about 4 nm,

the difference between the ground state energy levels obtained by using the parabolic model and the non-parabolic model is about 0.3 eV. For the radii larger than 14 nm, both the parabolic model and the non-parabolic models can give the same results. Figure 3(b) shows the ratio of $E(m)/E(0)$ as a function of QD radius, with the height fixed to be 5 nm. As can be seen, the dependence of the effect mass of InAs on energy is more sensitive than that of GaAs. So the ratio of wavefunction distribution in the well region to that in the barrier region would determine the influence degree of energy dependent effective mass.

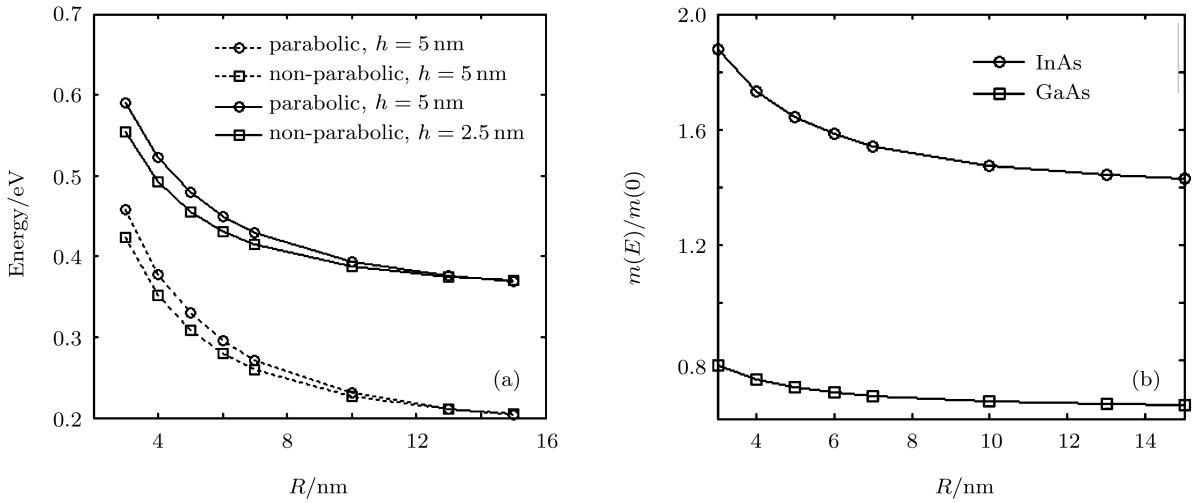


Fig.3. The curves for ground state energy level (a) and energy dependent effective mass (b) versus radius of parabolic and non-parabolic cylindrical QDs, with heights being 5 nm.

Figure 4 shows the ground energy levels as a function of the geometric size for rectangular cross-sectional QRs. As can be seen, when the inner radii of the QRs are fixed, the energy levels are not sensitive to the non-parabolic effects. The difference between the results calculated under the two conditions is not obvious. It should be noted from Fig.4(a) that for the QRs with an inner radius of 15 nm and a height of 5 nm, when widths of QRs are less than 15 nm, the energy levels calculated from the non-parabolic effective mass are less than those calculated from the parabolic effective mass. When widths of QRs are larger than 15 nm, the opposite results can be observed. However, in Fig.4(b), for the QRs with their inner radii and widths all fixed at 5 nm, the variation tendency is just the opposite. As can be seen, when heights are

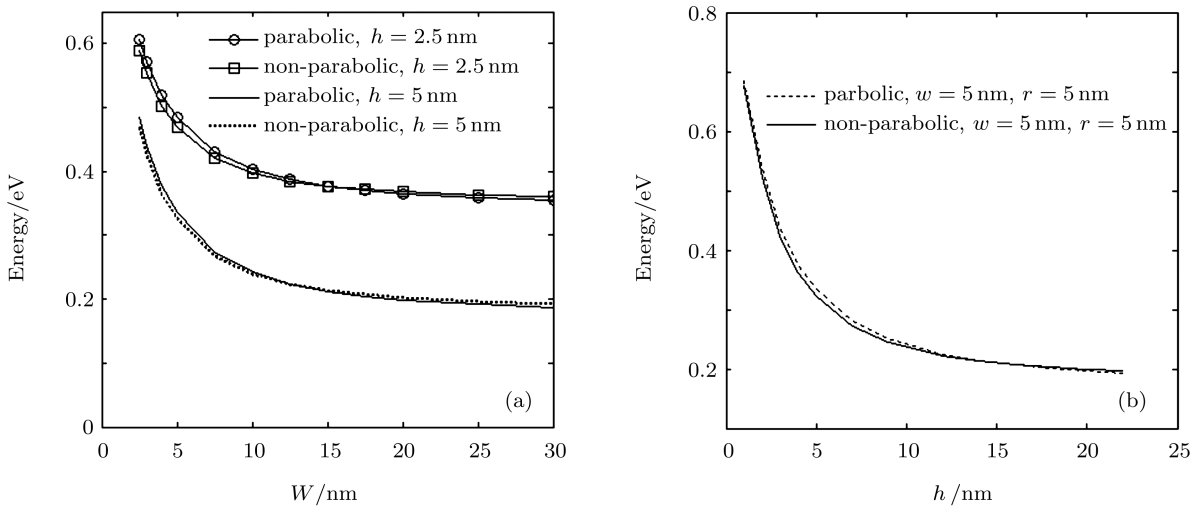


Fig.4. Curves for ground state electronic energy level as a function of size (width and height) of rectangle cross-section for parabolic and non-parabolic QRs, with their inner radii fixed at 20 nm (a), and a function of height of rectangle cross-section for parabolic and non-parabolic QRs, with their inner radii and widths all fixed at 5 nm (b).

less 15 nm, the ground energy levels calculated by using the parabolic effective mass are overestimated compared with those calculated by using the energy dependent effective mass. For heights larger than 15 nm, we can see the opposite circumstance. Without considering the influence of the inner radius, we can see from Figs.4(a) and 4(b) that there exists a maximum difference in energy level when the cross-sections of the rectangular QRs become square shaped. This phenomenon can be attributed to the fact that the energy dependent effective mass is very sensitive to the wavefunction distributions.

Figure 5 presents the calculated ground state energy levels of square cross-sectional QRs as a function of their inner radii. We can see the energy levels are very sensitive to the inner radii when the inner radii are less than 5 nm. This may arise from the enforced transverse coupling effects when the barrier becomes thinner with inner radius decreasing. However, the difference in energy level is mainly sensitive to height but not to inner radius. For example, the differences in energy level are about 0.01 and 0.02 eV when heights are 5 and 2.5 nm respectively.

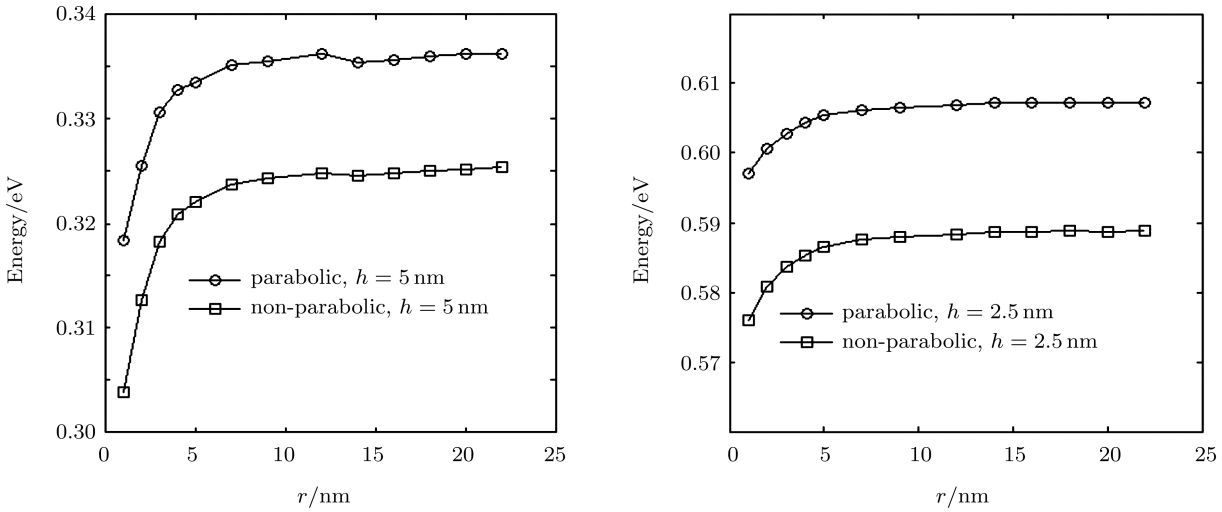


Fig.5. The dependences of ground state electronic energy level on the inner radius for square cross-sectional parabolic and non-parabolic QRs, with their heights being 5 nm (a) and 2.5 nm (b).

Figure 6 shows the ground energy levels as a function of inner radius for circular cross-sectional QRs. The radii of the circularity are 5 and 2.5 nm respectively. In spite of some similarities to Fig.5, we can see the most important difference is that when the inner radii are less than a critical value, the ground state

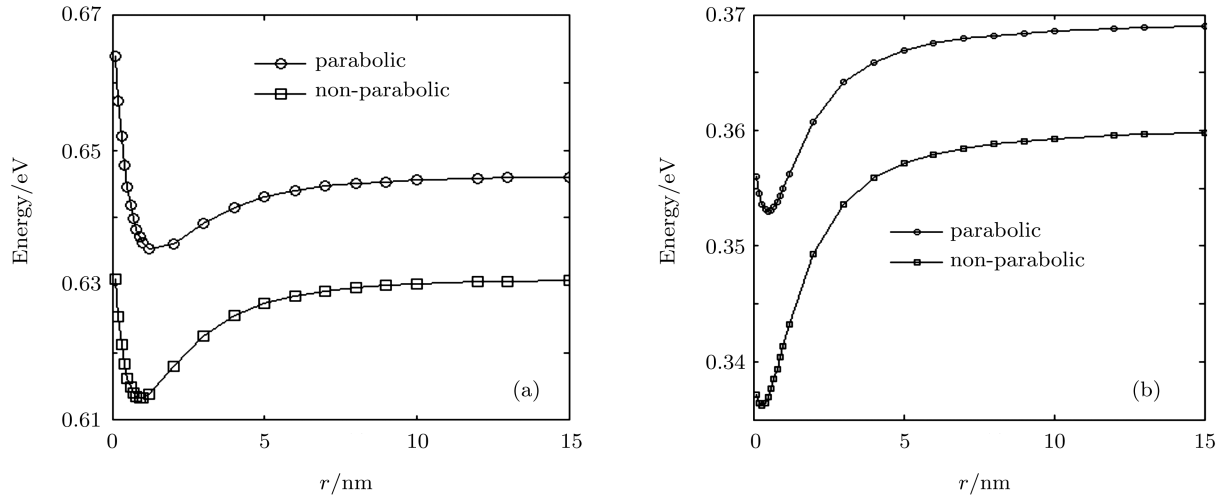


Fig.6. The dependences of ground state electronic energy levels on the inner radius of circular cross-sectional parabolic and non-parabolic QRs with their radii being 2.5 nm (a) and 5 nm (b).

energy levels will increase with inner radius decreasing. The smaller cross section area will correspond to a larger critical inner radius. For the values of circularity with radii of 2.5 and 5 nm, the energy level transition takes place when the critical values of the outer radii (radius is) are 1 and 0.4 nm respectively. The critical value is also dependent on the non-parabolic effect. We can see that the energy dependent effective mass will lead to a relatively smaller critical value than the calculated results by using the parabolic effective mass.

To explain the transverse coupling effects and the influence of the energy dependent effective mass, we show the wavefunction distribution ratio of the QR in the whole structure in Fig.7. The ratio is defined as $\int_{\Omega_{\rm well}} \psi {\rm d}s / \int_{\Omega_{\rm well}+\Omega_{\rm barrier}} \psi {\rm d}s$. We can see that the ratio will increase rapidly with inner radius decreasing on condition that the inner radius is less than 2 nm. This means the weaker coupling effects of the inner part of QR, when the QR is converted into a QD with the decrease of inner radius. As shown in Fig.3(b), the InAs material is more sensitive to the energy dependent effective mass. So with the enhanced size confinement effect when the inner radius decreases to less than 2 nm, the portability of finding the electron in the InAs region will increase, which further leads the influence of the energy dependent effective mass on energy levels to be strengthened.

Figure 8 shows the energy levels as a function of outer radius when the inner radius is 5nm and the height is 2.5 nm. The differences between the energy levels calculated by using the parabolic model and the non-parabolic models are also shown in Fig.8. We can see that both models give the same results when the outer radius is about 12 nm. For a larger outer radius the parabolic model overestimates the ground state energy levels, while for a smaller outer radius (less than 12 nm), the parabolic model underestimates the ground state energy levels. Their difference is less than ± 0.02 eV. Figure 8(b) shows the corresponding ratio of energy dependent effective mass to that of the bulk materials. The ratio of the wavefunction distribution of the QR in the whole structure is also shown. We can see that the ratio is not sensitive to the size of the QR when the outer radius is larger than 12 nm.

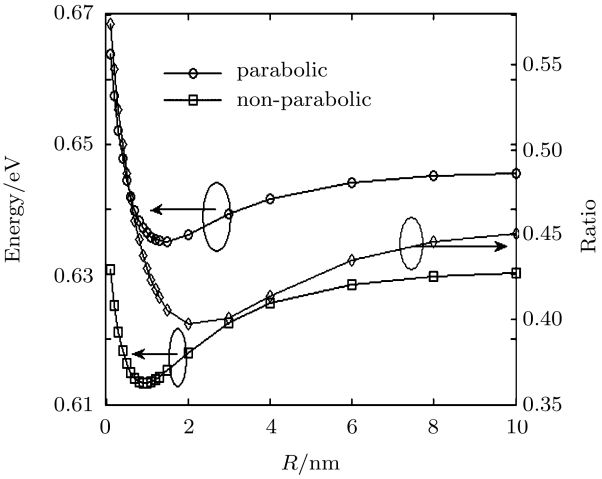


Fig.7. The portability of finding an electron separately in circular cross-sectional parabolic and non-parabolic QRs as a function of inner radius, with their outer radii being 2.5 nm.

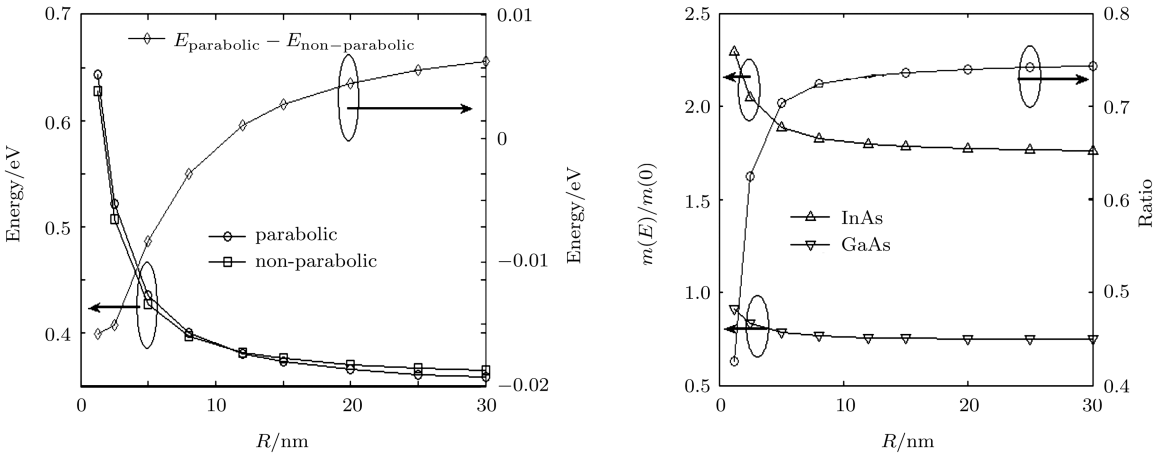


Fig.8. The dependences of energy level and effective mass on outer radius R, when the inner radius is 5 nm and the height is 2.5 nm, where (a) shows the energy levels with and without considering the non-parabolic effects, and (b) exhibits the values of energy dependent effective mass for InAs and GaAs and the wavefunction distribution ratio of the QR in the whole structure.

In the above, we have investigated the dependences of energy level and effective mass on parameters of QD and QR. However, there are some limitations in our simulation model. First, the strain effects and wetting layer are completely excluded from consideration in our model. In fact, they are very important for the performance of the devices.[16,17] and can be easily taken into consideration in our model, but at the expense of discarding the advantage of axial symmetry due to the anisotropic feature of the strain. Second, the more complex valence band intermixing effects are not included in our model. To take such effects into consideration, a complex multi-band effective mass theory should be used.[18] Third, the interaction among carriers is ignored in our model. If only the Coulomb effect is taken into consideration, it is easily to integrate this effect with our model, for the main algorithm of the Hartree approximation can be realized by iteration.[19] If the exchange and correction effects of the carriers are taken into consideration, one must use a more complex Hartree–Fock approximation or the density function theory (first-principles method),[20,21] and these methods are beyond the scope of the present study.

4. Conclusions

We investigate the ground state energy levels for the axially symmetric InAs/GaAs QD and QR. The analysis is detailed about the dependence of ground state energy level on geometric size parameters, such as inner radius, outer radius and height. For comparison, both the parabolic and non-parabolic effective mass models are employed in our calculation. The effect of geometric size on the energy dependent effective mass is discussed for QD and QR structures separately. We find that the effective mass is very sensitive to the wavefunction distribution ratio of a quantum well region in the whole structure; the wavefunction distribution is very sensitive to the geometric size. So the energy levels become more sensitive to the geometric size itself and its relevant effective mass. For the QR structure, there exists a critical inner radius, where the energy levels will have a transition that wanes with inner radius decreasing. This phenomenon may be attributed to the fact that strong coupling effects become weaker when the QR converts to a QD with inner radius decreasing. Although there are some limitations in our model, the simulated results reflect some guidelines for both the material fabrication and device design.[22−24]

References

[1] Masse N F, Homeyer E, Marko I P, Adams A R and Loualiche 2007 *Appl. Phys. Lett.* **91** 131113

[2] Jolley G, Fu L, Tan H H and Jagadish C 2007 *Appl. Phys. Lett.* **91** 173505

[3] Sugawara M, Ebe H, Hatori N, Ishida M, Arakawa Y, Akiyama T, Otsubo K and Nakata Y 2004 *Phys. Rev.* B **69** 235332

[4] Luis G G V, Dias D S, Jose M, Villas B and Sergio E U 2007 *Phys. Rev.* B **76** 155306

[5] Takuma Okunishi, Yusuke Ohtsuka, Masakazu Muraguchi and Kyozaburo Takeda 2007 *Phys. Rev.* B **75** 245314

[6] Yu L W, Chen K J, Song J, Xu J, Li W, Li X F, Wang J M and Huang X F 2007 *Phys. Rev. Lett.* **98** 166102

[7] Michael Sztucki and Till Hartmut Metger 2006 *J. Appl. Phys.* **99** 033519

[8] Kratzer P and Liu Q K K 2006 *Phys. Rev.* B **73** 205347

[9] Li S S, Xia J B, Yuan Z L and Xu Z Y 1996 *Phys. Rev.* B **54** 11575

[10] Mathiieu luisier, Andreas Schenk, Wolfgang Fichtner and Gerhard Klimeck 2006 *Phys. Rev.* B **74** 205323

[11] Williamson A J, Wang L W and Zunger Alex 2000 *Phys. Rev.* B **62** 12963

[12] Liu Y M, Yu Z Y and Huang Y Z 2006 *Int. J. Mod. Phys.* B **20** 4899

[13] Liu Y M, Yu Z Y, Huang Y Z and Yang H B 2006 *Acta Phys. Sin.* **55** 5023 (in Chinese)

[14] Liu Y M, Yu Z Y and Huang Y Z 2007 *J. University Sci. Technol.* (Beijing) **14** 477

[15] Liu Y M, Yu Z Y and Ren X M 2008 *Chin. Phys. Lett.* **25** 1850

[16] Markussen T, Kristensen P, Tromborg B, Berg T W and Mork J 2006 *Phys. Rev.* B **74** 195342

[17] Liu Y M, Yu Z Y and Ren X M 2008 *Chin. Phys.* B **17** 3471

[18] Chang K, Li S S, Xia J B and Peeters F M 2004 *Phys. Rev.* B **69** 235203

[19] Chang K, Xia J B and Peeters F M 2003 *Appl. Phys. Lett.* **82** 2661

[20] Jiang H, Baranger H U and Yang W T 2003 *Phys. Rev.* B **68** 165337

[21] Zhang Z Z Partoens B, Chang K and Peters F M 2008 *Phys. Rev.* B **77** 155201

[22] Jiao R Z, Feng C X and Ma H Q 2008 *Acta Phys. Sin.* **57** 1352 (in Chinese)

[23] Lin Y M, Yu Z Y and Yang H B 2005 *Opt. Commun.* **246** 367

[24] Jiao R Z and Feng C X 2008 *Acta Phys. Sin.* **57** 685 (in Chinese)